

High-pressure experimental and DFT structural studies of aurichalcite mineral

David Santamaría Pérez*

*Departamento de Física Aplicada-ICMUV, Universitat de València,
MALTA Consolider Team, 46100 Valencia, Spain*

Raquel Chuliá-Jordán

Departamento de Didáctica de las Ciencias Experimentales y Sociales, Universitat de Valencia, 46022, Valencia, Spain

A. Otero-de-la-Roza

*Departamento de Química Física y Analítica and MALTA-Consolider Team,
Facultad de Química, Universidad de Oviedo, 33006 Oviedo, Spain*

Robert Oliva

GEO3BCN – Geosciences Barcelona, CSIC, 08028, Barcelona, Spain

Catalin Popescu

CELLS-ALBA Synchrotron Light Facility, Cerdanyola del Vallés, 08290, Barcelona, Spain

(Dated: April 4, 2023)

RELATIVE STABILITY OF Zn_8/Cu_2 ATOMIC CONFIGURATIONS AT ZERO PRESSURE

The two phases examined in this manuscript, aurichalcite and hydrozincite, there are 10 positions over which the Zn and Cu atoms are distributed. The Zn/Cu proportion closest to experiment is Zn_8/Cu_2 , and therefore there are 45 possible arrangements of these atoms over a single unit cell. In order to analyse the phase stability under pressure, we first examine the relative stability of each of these arrangements at zero pressure upon geometry relaxation. The computational details for these calculations are given in the manuscript.

In the aurichalcite phase, the symmetry-unique Wyckoff positions of the parent space group are three $2e$ positions and one $4f$. Table S1 gives the relative energy, relative volume, and space group of each atomic arrangement in the aurichalcite structure at zero pressure upon geometry relaxation. The equivalent results for the hydrozincite phase, with three symmetry-unique positions ($2a$, $4h$, and $4i$) are shown in Table S2.

We studied the equations of state of the minimum-energy atomic configuration at zero pressure, labeled as “eq” in both tables. For comparison, we also considered the equations of state of two other atomic arrangements that have reasonably low energies at zero pressure and are more compact, in case one of them becomes more stable under pressure. These arrangements are entries “32” and “33” in the aurichalcite atomic configuration list (Table S1) and entries “8” and “19” in the hydrozincite list (Table S2). Following the computational procedure described in the main text, we calculated the energy-volume (Figure S1) and enthalpy-pressure (Figure S2).

The figures show that in the Zn_8Cu_2 composition, unlike for pure Zn, the aurichalcite phase is more stable than hydrozincite in the entire pressure range studied. Although the three hydrozincite configurations considered show more or less the same enthalpy *vs.* pressure behavior, the aurichalcite configuration with minimum energy at zero pressure is significantly more stable than the other two, and more stable than the three hydrozincite structures. Since, according to the enthalpy diagram, the minimum-energy arrangements of both phases at zero pressure are the most stable at all pressures, we consider only these two configurations in the main text.

TABLE S1. Energies and volumes per unit cell of the equilibrium geometries of the various Zn_8/Cu_2 atomic configurations in the **aurichalcite structure**, relative to the minimum-energy configuration. The self-consistent field process for the entries with “—” could not be converged. The four symmetry-unique positions and a set of representative coordinates are: A = $2e(0.238, 3/4, 0.931)$, B = $2e(0.610, 3/4, 0.116)$, C = $4f(0.2497, 0.4939, 0.4236)$, D = $2e_c(0.112, 1/4, 0.866)$. Column “Conf.” gives the placement of the two Cu atoms in the cell, and column “Sp. Grp.” is the resulting space group symbol (without hydrogens). The symbol in the first column indicates whether the equation of state has been calculated and the corresponding label used in the following figures. The “eq” label indicates the system studied in the main text.

	Conf.	$\Delta V(\text{\AA}^3)$	$\Delta E(\text{eV})$	Sp. Grp.
	A ₁ A ₂	3.572	0.637	P2 ₁ /m
	A ₁ B ₁	-0.488	0.530	Pm
	A ₁ B ₂	1.404	0.697	Pm
	A ₁ C ₁	—	—	P1
	A ₁ C ₂	—	—	P1
	A ₁ C ₃	2.146	0.309	P1
	A ₁ C ₄	—	—	P1
	A ₁ D ₁	-0.261	0.749	Pm
	A ₁ D ₂	0.477	0.972	Pm
	A ₂ B ₁	1.391	0.697	Pm
	A ₂ B ₂	-0.486	0.530	Pm
	A ₂ C ₁	—	—	P1
	A ₂ C ₂	1.346	0.284	P1
	A ₂ C ₃	—	—	P1
	A ₂ C ₄	2.161	0.305	P1
	A ₂ D ₁	0.478	0.972	Pm
	A ₂ D ₂	-0.266	0.749	Pm
	B ₁ B ₂	-0.035	0.758	P2 ₁ /m
	B ₁ C ₁	-0.121	0.310	P1
	B ₁ C ₂	0.156	0.401	P1
	B ₁ C ₃	0.147	0.401	P1
	B ₁ C ₄	-0.123	0.465	P1
	B ₁ D ₁	-0.009	1.091	Pm
	B ₁ D ₂	0.083	1.102	Pm
	B ₂ C ₁	0.150	0.401	P1
	B ₂ C ₂	-0.082	0.465	P1
	B ₂ C ₃	-0.081	0.310	P1
	B ₂ C ₄	-0.599	0.397	P1
	B ₂ D ₁	0.086	1.101	Pm
	B ₂ D ₂	-0.007	1.091	Pm
	C ₁ C ₂	-0.005	0.000	P $\bar{1}$
*(32)	C ₁ C ₃	-0.615	0.033	P2 ₁
*(33)	C ₁ C ₄	-1.281	0.171	Pm
	C ₁ D ₁	—	—	P1
	C ₁ D ₂	-1.494	0.674	P1
	C ₂ C ₃	-1.265	0.171	Pm
	C ₂ C ₄	-0.610	0.033	P2 ₁
	C ₂ D ₁	-1.492	0.674	P1
	C ₂ D ₂	—	—	P1
*(eq)	C ₃ C ₄	0.000	0.000	P $\bar{1}$
	C ₃ D ₁	-1.499	0.674	P1
	C ₃ D ₂	—	—	P1
	C ₄ D ₁	—	—	P1
	C ₄ D ₂	-1.502	0.840	P1
	D ₁ D ₂	-0.102	1.414	P2 ₁ /m

TABLE S2. Energies and volumes per unit cell of the equilibrium geometries of the various Zn_8/Cu_2 atomic configurations in the **hydrozincite structure**, relative to the minimum-energy configuration. The self-consistent field process for the entries with “—” could not be converged. The three symmetry-unique positions and a set of representative coordinates are: $A = 2a(0, 0, 0)$, $B = 4h(0, 0.263, 1/2)$, $C = 4i(0.129, 1/2, 0.038)$. Column “Conf.” gives the placement of the two Cu atoms in the cell, and column “Sp. Grp.” is the resulting space group symbol (without hydrogens). The symbol in the first column indicates whether the equation of state has been calculated and the corresponding label used in the following figures. The “eq” label indicates the system studied in the main text.

	Conf.	$\Delta V(\text{\AA}^3)$	$\Delta E(\text{eV})$	Sp. Grp.
	A_1A_2	—	—	$C2/m$
	A_1B_1	0.009	0.169	P2
	A_1B_2	0.978	0.209	P2
	A_1B_3	-0.181	0.234	P2
	A_1B_4	—	—	P2
	A_1C_1	0.129	0.392	Pm
	A_1C_2	0.102	0.669	Pm
*(8)	A_1C_3	-2.567	0.332	Pm
	A_1C_4	0.388	0.663	Pm
	A_2B_1	—	—	P2
	A_2B_2	1.984	0.149	P2
	A_2B_3	—	—	P2
	A_2B_4	5.607	0.093	P2
	A_2C_1	-1.536	0.456	Pm
	A_2C_2	0.199	0.357	Pm
	A_2C_3	-2.056	0.553	Pm
	A_2C_4	-0.069	0.365	Pm
	B_1B_2	2.762	0.027	C2
*(19)	B_1B_3	-0.875	0.078	$P2/m$
	B_1B_4	-0.723	0.167	$P2/c$
	B_1C_1	0.825	0.241	P1
	B_1C_2	4.792	0.411	P1
	B_1C_3	1.927	0.288	P1
	B_1C_4	2.118	0.447	P1
	B_2B_3	-0.331	0.151	$P2/c$
*(eq)	B_2B_4	0.000	0.000	$P2/m$
	B_2C_1	0.891	0.320	P1
	B_2C_2	-0.629	0.383	P1
	B_2C_3	-0.893	0.514	P1
	B_2C_4	-0.333	0.406	P1
	B_3B_4	-0.440	0.195	C2
	B_3C_1	1.704	0.233	P1
	B_3C_2	6.752	0.438	P1
	B_3C_3	-2.483	0.338	P1
	B_3C_4	-0.201	0.555	P1
	B_4C_1	0.135	0.327	P1
	B_4C_2	-0.725	0.382	P1
	B_4C_3	-1.143	0.495	P1
	B_4C_4	-0.791	0.369	P1
	C_1C_2	2.114	0.747	Cm
	C_1C_3	-0.931	0.753	$P2/m$
	C_1C_4	-0.040	0.632	$P2_1/m$
	C_2C_3	-0.843	0.834	$P2_1/m$
	C_2C_4	3.188	0.815	$P2/m$
	C_3C_4	—	—	Cm

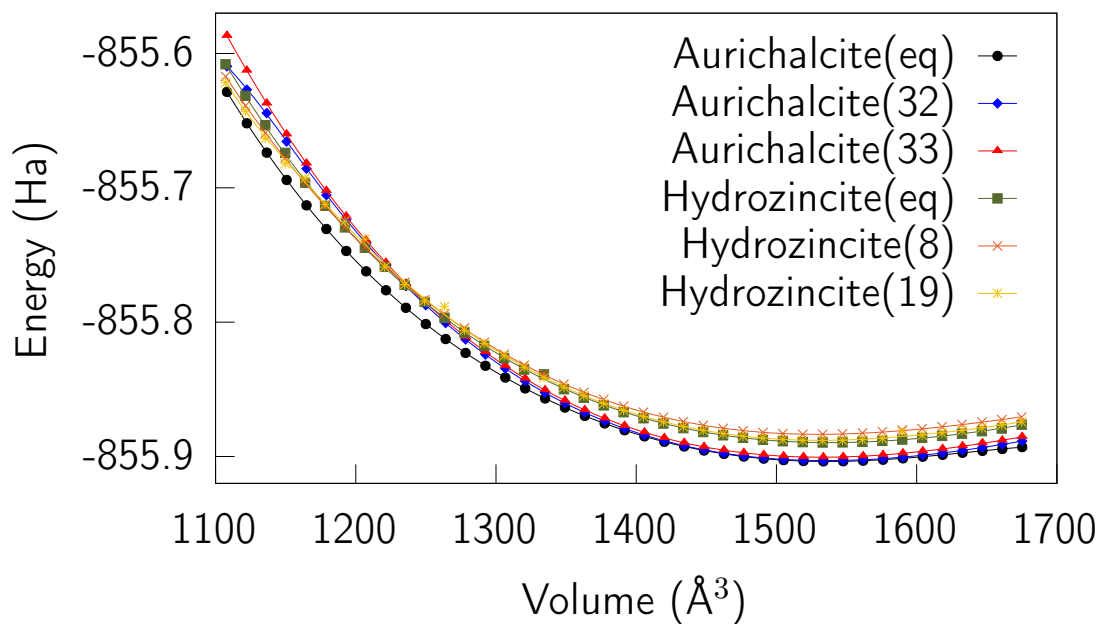


FIGURE S1. Energy *versus* unit cell volume for the three aurichalcite and hydrozincite structures considered.

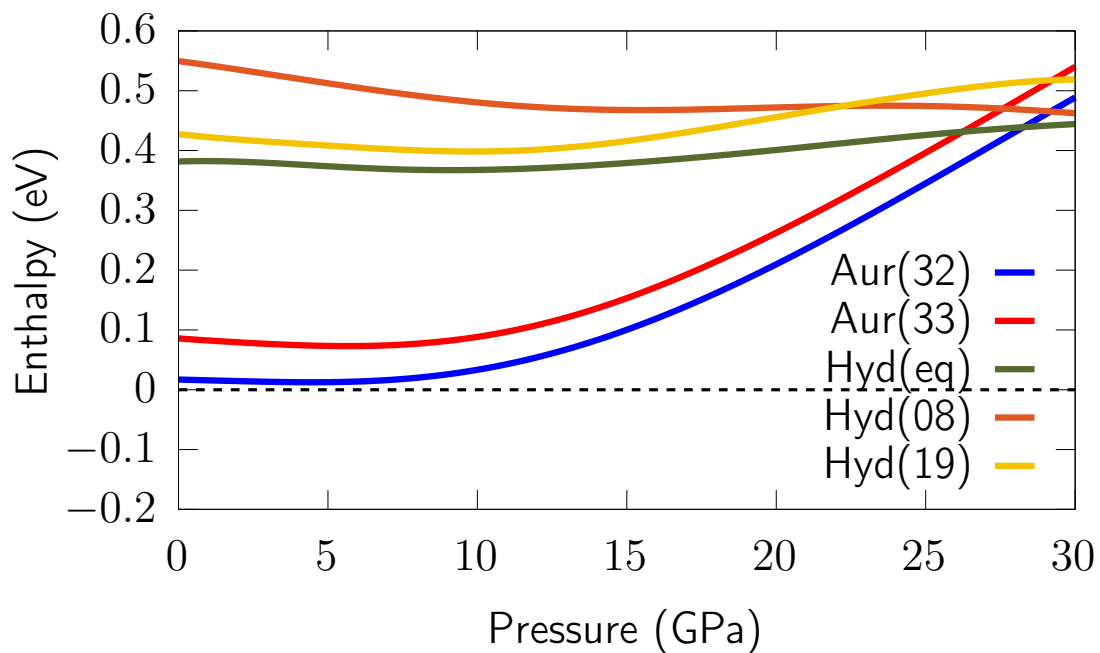


FIGURE S2. Enthalpy *versus* pressure for the three aurichalcite and hydrozincite structures considered, relative to the enthalpy of the minimum-energy aurichalcite structure, which corresponds with the $y = 0$ axis.

TRICLINIC STRUCTURE AT HIGH PRESSURES

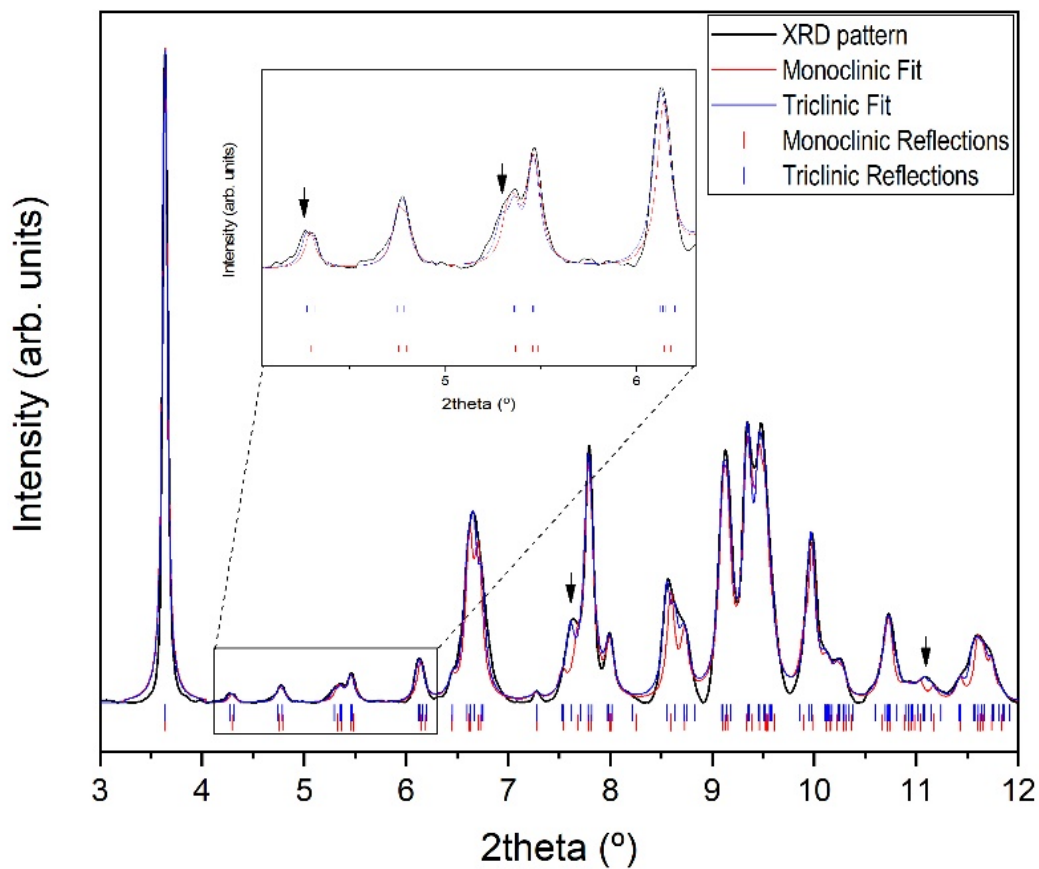


FIGURE S3. Experimental XRD pattern at 5.4 GPa (in black). Red and blue lines represent the LeBail fits using the initial $P2_1/m$ monoclinic unitcell and a less symmetric $P\bar{1}$ triclinic unitcell, respectively. It can be seen that the monoclinic cell cannot explain all the diffraction peaks of the pattern (see arrows, for instance) and that the triclinic structure provides a reasonable fit.